# Assessment of the Complex Refractive Indices of Xenopus Laevis Sciatic Nerve for the Optimisation of Optical (NIR) Neurostimulation

Enayetur Rahman, Michael B. Powner, Panayotis A. Kyriacou and Iasonas F. Triantis

***Abstract*—Despite an increasing interest in the use of light for neural stimulation there is little information on how it interacts with neural tissue. The choice of wavelength in most of the optical stimulation literature is based on already available light sources designed for other applications. This paper is the first one to report the complex refractive index of the *Sciatic* nerve of *Xenopus laevis*, which is a crucial parameter for identifying the optimal wavelength of optical stimuli. The *Xenopus laevis* neural tissue is the most widely used tissue type in peripheral neurostimulation studies. In this work, the Reflectance ($R$) and the Transmittance ($T$) of the *Sciatic* nerve were measured over a wavelength range of 860 nm to 2250 nm, and the corresponding real ($n$) and the imaginary ($k$) refractive indices were calculated using appropriate formulae in a novel way. The reported $n$ values were between 1.3-1.44 and the $k$ values are of the order of $10^{-5}$ over the full wavelength range. The absorption coefficient, $\alpha$ was found to be 100-500 cm$^{-1}$. Several localised wavelength ranges were identified that can offer a maximised power coupling between potential optical stimuli and the neural tissue (1150-1200 nm, 1500-1700 nm and 1900-2050 nm). The narrower regions of 1400-1600 nm and 1850-2150 nm were found to exhibit maximised absorbance. Separately, three regions were identified, where the penetration depths are the greatest (950-1000 nm, 1050-1350 nm and 1600-1900 nm). This paper provides, for the first time, the fundamental specifications for optimising the parameters of optical neurostimulation systems.**

***Index Terms*—Spectrophotometry, Neurostimulation, Optical Stimulation, *Sciatic* nerve, Complex refractive index, *Xenopus laevis*.**

## I. Introduction

ARTIFICIAL stimulation of peripheral nerves, either for activation or for inhibition or blocking has an increasing range of therapeutic applications, respectively ranging from restoration of function by functional electrical stimulation (FES) following spinal cord injury (SCI) [1]–[3] to pain relief and seizure suppression action in treatment-resistant epilepsy [4]. Electrical Nerve Stimulation (ENS) is the benchmark modality for artificial intervention to neural signalling and altering stimulus waveform parameters in combination with electrode topology variations allow its use towards either the generation of action potentials (AP) - e.g. with well reported biphasic waveforms [5] - or towards stopping ongoing neural activity - e.g. through the use of high-amplitude long duration pulses or high-frequency waveforms [6]. Although some very well performing systems have been presented [3], [5], [7]–[13], there are still some challenges that ENS has not addressed satisfactorily i.e. limited fascicle selectivity due to poor localization or lack of directional selectivity - the separate addressing of afferent and efferent pathways [14], and the presence of stimulus artefacts [15]. As a result the therapeutic potential of artificial neurostimulation cannot be reached by the current ENS methods alone, as their use entails side-effects including the activation of non-targeted structures and the inability to fully block neural activity when required.

Optical and more specifically Infrared Nerve Stimulation (INS) of unmodified peripheral nerves (as opposed to the case of Optogenetics [16]) is increasingly been considered as an alternative or a complementary modality to electrical neurostimulation as it has the potential to offer a much more localised and thus selective effect. Recent studies [17]–[19] have investigated the effects of light in stimulating peripheral and central nervous system (PNS and CNS) tissue, mainly exploring wavelengths in the Near Infra-red (NIR) region of the light spectra [17], [19]. Similar to its electrical counterpart, optical stimulation has been shown to achieve neural activation [10], [18], [20], [21] and blocking [22], with both effects attributed to localized temperature rise due to infrared radiation absorption by water molecules. Literature indicates that such a temperature increase affects mechanisms such as ion channel gating; activation of intracellular second messenger; formation of membrane pores; increase of conductances; or triggering of thermo-resistive ion-channels [23].

The differences between the optical stimuli that generate or block action potentials (AP) have been reported to relate to stimulus pulse duration. One recent study [23] that examined the underlying mechanism for neural activation, indicated that a short duration high energy infrared pulse results in an increase in the membrane capacitance and thereby generates a depolarizing current. Similarly, the first work that reported blocking neural signals in excited neurons using INS [22] indicated that a local heat increase due to a LASER irradiating a specific node of Ranvier for a prolonged duration blocks APs from passing through it and makes that node resistant to starting a new AP.

These studies assess the response of neurons by measuring the light's effect on neural activity experimentally and by confirming the thermal effect through simulation [22]. However, to the authors' knowledge, the optimum wavelengths for optical neurostimulation are yet to be determined, while the exact nature of the interaction of light with neural tissue and

Dr E. Rahman is with the NIBEC, School of Engineering, Ulster University, Prof. P.Kyriacou and Dr I. Triantis are with the Department of EEE and Dr M. Powner is with the Centre for Applied Vision Research at City, University of London, UK. E-mails: [e.rahman@ulster.ac.uk, enayet.rahman / michael.powner / p.kyriacou / i.triantis] @city.ac.uk

the optical energy or the optical parameters that are required to reach deep fascicles or fibres when optical stimulation is applied extraneurally to a nerve bundle have not been investigated in detail. Most of the aforementioned studies use LASERs with wavelengths ranging between 1550 nm [22] - the popular wavelength for optical communication - and 1850 nm [19]. Still, lack of information regarding the optical constants of neural tissue over the entire NIR spectrum makes it difficult to determine if the choice of a specific wavelength is optimum for either inhibition or excitation and what is the depth of penetration in neural tissue, especially in peripheral nerves.

Given optical stimulation's potential for localization and hence selectivity - either fascicular or directional - which could lead to minimization of any side-effects during optical or mixed-mode stimulation, it is very desirable to carry out research that will determine the optical parameters of neural tissue over the NIR spectrum. The optical energy distribution and absorption in the nerve can be characterized by the real and imaginary parts of the refractive indices of the nerve. To be able to selectively stimulate, block or inhibit specific nerve fibres it is imperative to investigate the propagation and depth of penetration of an optical signal through the various layers of a peripheral nerve.

This paper aims to offer new insights into the interaction of light with neural tissue (similar to the illustration in Fig. 1) by determining the complex refractive indices of the *xenopus laevis sciatic* whole nerve bundle in the NIR region and more specifically in the wavelength range of $860 - 2250$ nm, using spectrophotometry and custom modified mathematical formulae.

*Xenopus sciatic* tissue is commonly used for neuroprostheses research [24] and the choice of wavelength range is for consistency with all relevant literature, where water is indicated as the dominant IR absorber, with very little absorbance in the visible spectrum. The water content of nerves as reported by [25] is about $55\%$. By determining the absorption coefficient of the entire nerve, it is possible to determine if the remaining $45\%$ content of the neuron has any distinctive absorption characteristics present or not. Determination of the optical constants from acquired spectrophotometric data requires the formulation of an inverse problem [26], where the real ($n$) and imaginary ($k$) parts of the refractive indices can be determined from the measured Transmittance($T$) and Reflectance ($R$) data determined experimentally through the use of a Spectrophotometer on neural tissue samples. The problem in determining the optical constants from $R$ and $T$ for a sample with finite thickness is that there are multiple reflections within the sample, which alters the obtained values of $n$ and $k$ by as much as $80\%$ [27]. To avoid such inaccuracies in obtaining the optical constants, the formalism by Airy and Abelès [26] that accounts for the multiple reflections within the sample is used in this paper.

Section II describes the method of sample preparation and the method of obtaining the optical constants from the measured spectrophotometric data. The results and discussions are given in Section III, and the conclusions are provided in Section IV.

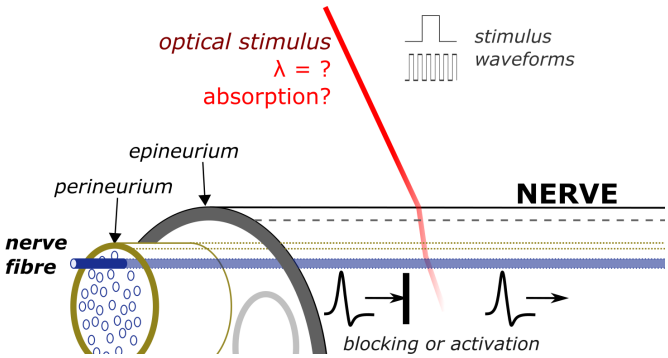


Fig. 1: Optical stimulus applied to a nerve bundle. Optical parameters will define whether it can reach deep fascicles and fibres and how it affects neural tissue.

## II. Methods

Spectrophotometric experiments were carried out on *Xenopus laevis* sciatic nerve samples using a PerkinElmer Lambda 1050 spectrophotometer. A 100 mm Integrating sphere (PerkinElmer) was used to capture all the scattered light within the sample. Appropriate formulae were used and modified to calculate optical parameters ($n,\ k$) from the spectrophotometric measurements ($R,\ T$), while eliminating the influence of the glass slide and the scattering.

### A. Sample Preparation

Ten *sciatic* nerve tissues were collected from five mature female *Xenopus laevis* subjects as detailed in table I. All animals were treated in accordance with the Animal Welfare Act 2006. The subjects were concussed by striking the back of the head and immediately culled by decapitation and destruction of the brain. The sciatic nerve was dissected from the base of the spine to the knee. The nerve was dissected away and isolated from the animal. The nerve was kept moist using standard amphibian Ringer solution [28].

The use of the animal samples in this study was approved by the Senate Research Ethics Committee of City, University of London.

TABLE I: Sample table

| Sample | Weight (g) | Sex |
|---|---|---|
| 1 | 180 | F |
| 2 | 195 | F |
| 3 | 195 | F |
| 4 | 175 | F |
| 5 | 200 | F |

The extracted nerve samples were sliced and placed between microscope glass slides that were especially shaped to fit within the Spectrophotometer sample chamber. At the same time, as proposed by the instrument manufacturer, a separate plain glass slide was placed in the reference path of the Spectrophotometer to eliminate the effects of the glass slides in the measurements. Removing the influence of the glass material from the measurements, allows for the assumption that the nerve sample is surrounded by air as shown in

fig. 2. This again, is the proposed practice by PerkinElmer, whereby when a sample immersed in a material is inserted in the instrument, that material can be placed in the reference chamber and measurements can then be assumed to correspond to the sample surrounded by air alone. Fig. 2 shows the sample, with thickness '$d$', interrogated by the spectrophotometer. The light intensity normally incident on the sample is $I_0$, the transmitted light intensity is $I_T$ and the reflected light intensity is $I_R$.

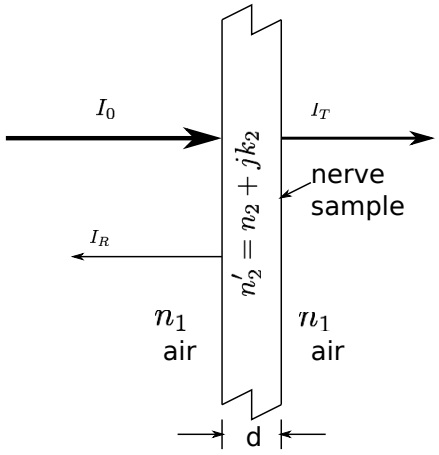


Fig. 2: Diagrammatic representation of the nerve sample inserted in the Spectrophotometer. Using a glass slide in the instrument's reference chamber allows for the outside medium to be considered as 'air' with a refractive index, $n_1 = 1$. The refractive index of the nerve sample can be expressed by a complex number as follows: $n_2' = n_2 + jk_2$

### B. Spectrophotometric Set-up

For spectrophotometric measurements, a Lambda 1050 dual beam UV/Visible/NIR spectrophotometer (Perkin Elmer Inc.) was used with a spectral region of $860 - 2250$ nm, covering most of the NIR region. Data was taken at 1 nm intervals. A Deuterium lamp was used as the source, while as detector an Indium Gallium Arsenide detector ($InGaAs$) was used. Slit settings for the NIR were set on *'Servo'* mode, and the NIR ($InGaAs$) gain of 11 was used. The response time for the detector was set at 0.2 seconds. The front and rear attenuators were set at $100\%$ for both the sample and reference beams. Baseline corrections ($100\ \%T/0A$ and $0\%T/blocked\ beam$) were performed to remove '*Background noise*' and help reduce the effects of any stray light in the system before placing the samples in the spectrophotometer. The '*CBM*' (Common Beam Mask) parameter was set at $100\%$, and the other spectrophotometer parameters were kept at their *'default'* values. The Detector module of the spectrophotometer was replaced by a $100\ mm$ Integrating sphere (Perkin Elmer Inc.). The sphere featured a reference compartment (Fig. 3) and a sample compartment and included white plates to disable these compartments when their use was not required. A reference empty slide was placed at the reference compartment (Fig. 3) for both $\%T$ (Transmittance) and $\%R$ (Reflectance) measurements. The white plate was kept at the *'sample compartment for R'* during the Transmittance and Absorbance measurements, while the sample slide replaced it during the Reflectance measurement. The sample slide was placed in the *'Sample compartment for T'* while measuring Transmittance and this compartment was left empty during Reflectance measurements. To obtain

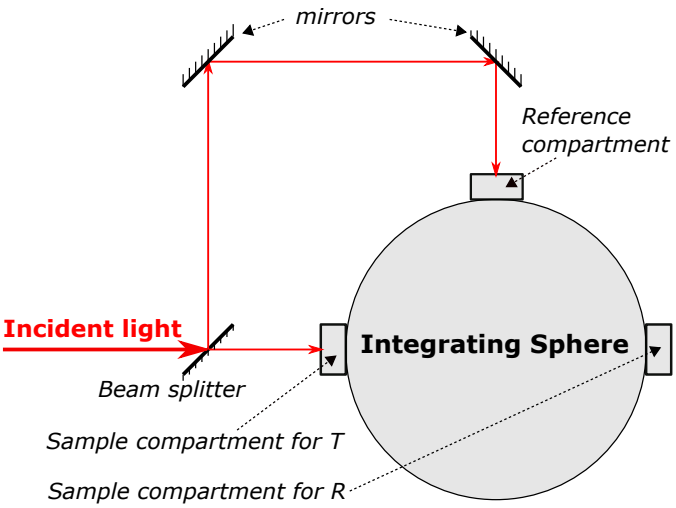


Fig. 3: Diagrammatic representation of an Integrating Sphere.

the optical constants ($n$, $k$ and $\alpha$) for the neural tissue, the spectrophotometer was used to determine the Transmittance ($T$) and Reflectance ($R$) for a sample with a thickness $d = 0.2\ mm$ over the wavelength range specified earlier. The Integrating Sphere (IS) was used to minimise the effects of scattering through the turbid medium on the measurements of $T$. For the modified expressions for $T$ and $R$ as given in equations (6) and (7) to be valid, the assumptions $d >> \lambda$ and $\Delta\lambda > \Delta\delta$ were made, where $\Delta\lambda$ is the difference between the consecutive $\lambda$ values and $\Delta\delta$ is the line-spread of the spectrophotometer. Here, the value of $d \approx 0.2\ mm$ is much higher than the $\lambda \in [860\ nm - 2250\ nm]$ and the line-spread of the spectrophotometer was maintained to satisfy the second assumption. The extracted nerve sample was placed inside a container with the predefined thickness embedded into two glass slides. The measured $T$ and $R$ values were then used to approximate the first guess for Newton's iterative method to find the values of $k$ and $n$ by using equations (8) and (9). After a few iterations, the method converges towards the solution with user defined error tolerance. Once we obtained the value for $k$, $\alpha$ was determined by using equation (2).

### C. Determination of the Optical Constants

The optical properties of any homogeneous medium can be characterized by the complex refractive index. The refractive index of any medium can be expressed as:

$$n'(\lambda) = n(\lambda) + jk(\lambda) \tag{1}$$

here, $n$', $n$ and $k$ are the complex, real part and imaginary part of the refractive index at the wavelength $\lambda$. The imaginary part of the refractive index, $k$, is responsible for the optical absorption, where the absorption coefficient is given by:

$$\alpha(\lambda) = \frac{4\pi}{\lambda} k(\lambda)\ cm^{-1} \tag{2}$$

here, $\lambda$ is the free space wavelength in cm. The optical absorbance, $A$ can be given as:

$$A = \alpha(\lambda)d \tag{3}$$

here, $d$ is the optical distance.

$$I_d = I_0 e^{-\alpha(\lambda)d} \tag{4}$$

Here, $I_0$ is the initial light intensity and $I_d$ is the light intensity after propagating a distance 'd' through the medium. The Absorbance, A ($\alpha d$) becomes 1, when the intensity falls to $36.7\%$ of its initial value. We can consider that beyond this distance no considerable optical power is reached and therefore, we consider this distance as the penetration depth throughout this article. The real part of the refractive index ($n$) plays a role in controlling the refraction and reflection at the material interfaces. This study is not concerned about the refraction experienced by the optical signal within the nerve. However, the launched optical signal experiences reflection at the nerve boundary. Thus, an optical stimulation system would need to be designed so as to minimise that reflection as much as possible.

When light enters from one medium to another, due to the differences in the refractive indices ($\Delta n$) a certain amount of optical power is reflected back to the first medium, which is proportional to $\Delta n$. At a specific wavelength, $\lambda$, $\Delta n$ has to be minimized and $\alpha$ has to be maximized. The condition for $\Delta n$ will ensure that the optical power enters into the nerve with minimum Reflectance. A higher $\alpha$ will make sure that the entered optical power is absorbed into the inner material of the nerve to maximize the temperature rise.

Obtaining the optical constants ($n,\ k$) over the aforementioned spectral region will allow for the identification of the optimum wavelength or wavelengths for optical neurostimulation. Biological media generally have strong scattering properties. In this study, we are interested only in absorption. However, determination of the optical constants ($n,\ k$) is affected by the presence of scattering. Therefore, it is necessary to have a technique that eliminates or reduces the effects of scattering in obtaining the optical constants. That was the reason that the aforementioned Integrating Sphere (IS) was used in this study to remove the effects of scattering in the collected transmitted signal, which is used to calculate the optical constants.

As mentioned previously, the medium surrounding the sample was considered to be *'air'* with a refractive index of $n_1 = 1$, and the refractive index of the sample was $n_2'$ that is $n_2' = n_2 + jk_2$, where, $n_2$ is the real part of the refractive index and $k_2$ is the imaginary part of the refractive index of the nerve sample. The Reflectance at the medium air-nerve (1-2) interface can be written by Fresnel's equations as follows:

$$R_{12} = \frac{(n_2 - n_1)^2 + k_2^2}{(n_2 + n_1)^2 + k_2^2} \tag{5}$$

There are several methods available in the literature to determine the Optical constants from the measured Transmission and Reflection spectra [29], [30], [31], [27], [32], [33]. When it comes to determining the optical properties of biological samples a major issue is sample preparation, as the sample has to be embedded into glass or Quartz slides. The finite thickness of the sample introduces multiple reflections within the sample, reducing the reliability of the values produced by the traditional Beer-Lambert based calculation. By using the formalism of Airy and Abelès [26] the problem related to the multiple reflections within the sample can be reduced and as a result the Transmittance ($T$) and the Reflectance ($R$) can be expressed by the following equations:

$$T = \frac{I_T}{I_0} = \frac{(1 - R_{12})^2 e^{-\alpha d}}{1 - R_{12}^2 e^{-2\alpha d}} \tag{6}$$

$$R = \frac{I_R}{I_0} = R_{12} + \frac{R_{12}(1 - R_{12})^2 e^{-2\alpha d}}{1 - R_{12}^2 e^{-2\alpha d}} \tag{7}$$

where,

$$\alpha = \frac{4\pi k_2}{\lambda}$$

The absorption coefficient $\alpha$ is dependent on the imaginary part of the refractive index, $k_2$ and the wavelength, $\lambda$ of the incident light. The $T$ and $R$ values obtained from the spectrophotometer are functions of $n_2$, $k_2$, $d$, and $\lambda$ if we consider that $n_1 = 1$. So, in functional form, $T$ and $R$ can be expressed as $T(n_2, k_2, d, \lambda)$ and $R(n_2, k_2, d, \lambda)$. For specific, fixed $d$ and $\lambda$ they can be expressed as $T(n_2, k_2)$ and $R(n_2, k_2)$. We have now two non-linear equations with two unknowns ($n_2$, $k_2$) for each wavelength. Newton's iterative formula for solving non-linear equations of multiple variables can be used to determine the $n_2, k_2$ from the $T$ and $R$ obtained from the spectrophotometer. The initial values for the iterations of $k_2$ and $n_2$ can be determined as follows [26], [27]:

$$k_{2(ini)} = \frac{-ln(T + R) \times \lambda}{4\pi d} \tag{8}$$

$$n_2(ini) = \frac{(1 + R) + \sqrt{(1 + R)^2 - (1 - R)^2(k_{2(ini)}^2 + 1)}}{1 - R} \tag{9}$$

Newton's iterative method converges towards the actual solution and the initial estimate does not necessarily have to be very close to the target value ($\pm(20\ to\ 30)\%$) [34]. Under the assumptions made, the algorithm converges to the theoretical value predicted by the equations to the target tolerance set by the user. For the values used in this paper and with an error tolerance of the order of $10^{-10}$, it takes 4-5 iterations to reach the solution.

## III. Results and Discussion

Transmittance ($T$) and Reflectance ($R$) were obtained for the ten samples from the toad sample given in Table I by using PerkinElmer Lambda 1050 spectrophotometer equipped with a 100 mm IS following the procedure described in Section II. Figure 4 shows the average $T$ and $R$ for samples with a thickness of 200 $\mu m$ over the wavelengths 860 $nm$ to 2250 $nm$. The figure shows that the average Transmittance is about $90\%$ in the wavelength range and the average Reflectance is about $4\%$. As the summation of the Transmittance and Reflectance is not $100\%$, it indicates that the nerve samples possess about average $6\%$ absorbance. It is also clear that both the Transmittance and Reflectance spectra has two distinct

minima at around 1480 $nm$ and 1980 $nm$. The transmission spectra is fairly flat in the region $980 - 1380$ $nm$ with a $T \approx 0.93$. There is another wavelength range where the transmission is maximized that is $1600 - 1800$ $nm$. For neural stimulation, where the optical power source is external to the targeted tissue, is desirable to maximise transmittance while minimising reflectance to ensure maximum energy transfer from the source to the tissue. Thus, it is interesting to note that between the wavelengths of $1100 - 1380$ $nm$ the Reflectance has a flat region without being at its maximum value while the corresponding value for Transmittance is optimal.

Figure 5 (top) is the average real refractive index ($n$) as calculated by using the data of fig. 4 and equations (6) and (7). Error bars indicate the standard deviation of the biological samples as detailed in table I from all valid experiments. The graph exhibits two prominent local minima (1480 nm and 1980 nm), which corresponds to wavelengths for which optical power reflection is minimized. These $\lambda$ ranges need to be examined in conjunction with $\lambda$ where absorbance in the nerve tissue is maximum. Considering the fact that the real refractive index of the outer medium of the nerve being $\approx 1.3$ for the wavelengths 980 $nm$, 1480 $nm$ and 1980 $nm$ the Reflectances are 0.23, 0.009 and 0.0003 respectively. For the wavelength ranges of $1100 - 1380$ $nm$ and $1700 - 1850$ $nm$, 0.08% power will be reflected back.

Therefore, to maximize the optical power coupled to the nerve medium, the optimum choice of wavelength is either at around 1480 $nm$ or 1980 $nm$ considering only the effects of the real refractive index in the wavelength range. Still, either of $1100 - 1380$ $nm$ or $1700 - 1850$ $nm$ regions can be used if a broader wavelength operating range is required. As mentioned previously, an optical neurostimulation system utilises the optical power absorbed in the neural medium to raise the localised temperature. Thus, in order to identify the stimulator's optimum operating wavelength, the characteristics of the imaginary parts of the refractive indices ($k$) should be considered in conjunction with the real part ($n$).

In stimulating a nerve with IR radiation, the optical power emitted by a light source (Lasers or LED) has to be launched from outside the nerve boundary. As at an interface of two materials, where the refractive index changes a certain amount of optical power is reflected back into the medium from where the power is launched that because of Fresnel's reflection. The higher the refractive index difference ($\Delta n$), the higher the amount of power reflected. As the power transmitted into the nerve is of use for affecting the stimulation process, it is essential that the Transmittance be maximized. Figure 6 shows the reflected power from the nerve interface considering that the optical power is launched from a medium with a refractive index equals to that of water in the range $860$ $nm < \lambda < 2250$ $nm$. The Reflectance characteristics shown in fig. 4 clearly show that for the $1150$ $nm < \lambda < 1200$ $nm$ range the reflected power is minimum, which is desirable for optical stimulation. There are two more $\lambda$ ranges where the Reflectance is minimized, one in the range $1500 - 1700$ $nm$ and the other in $1950 - 2050$ $nm$. These two ranges can be the potential $\lambda$ for any optical nerve stimulation system as they ensure minimal reflections from the nerve boundary. There are

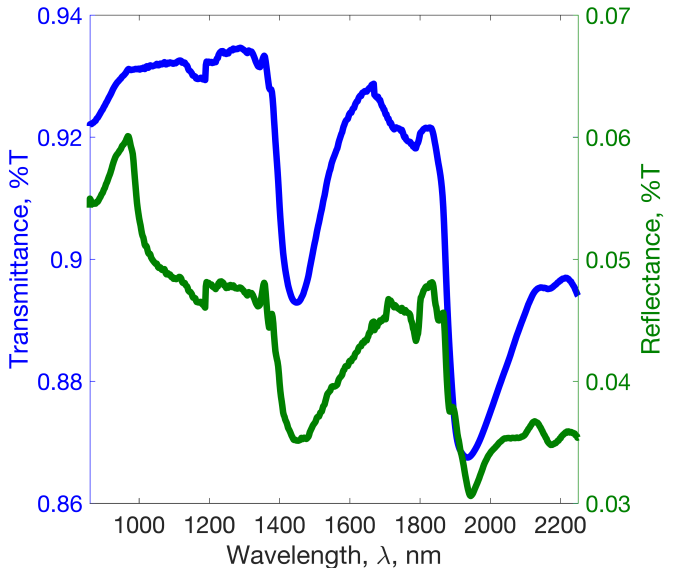


Fig. 4: Transmittance/Reflectance values of sciatic nerve of Xenopus laevis in NIR wavelengths with the Integrating Sphere

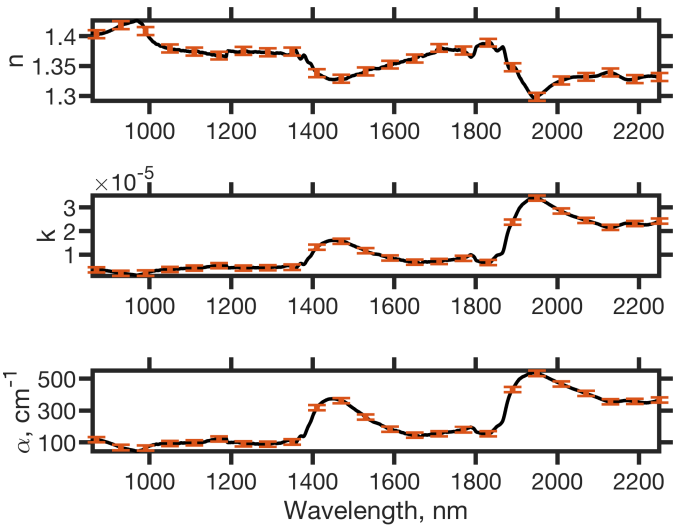


Fig. 5: Average real refractive index ($n$, top), imaginary refractive index ($k$, middle) and absorption coefficient ($\alpha$, bottom ) as calculated using the data of fig. 4 and Newton's iterative method

some wavelength ranges ($1250 - 1400$ $nm$ and $> 2050$ $nm$) that exhibit higher Reflectance from the nerve boundary, thus, optical stimulation launched at these wavelengths will experience higher reflected power (as high as 13%), resulting in poor power coupling. For such a system to operate efficiently, the system designer has to make sure that the reflected power is minimized either by choosing an appropriate wavelength range or by using a coupling material to minimize the impedance mismatch. Figure 5 (middle) shows the calculated imaginary refractive index ($k$), indicating $\lambda$ ranges that provide insight into the absorbance characteristics of the nerve tissue over the wavelength range. As discussed previously in Section II that the imaginary part of the refractive index is related to the

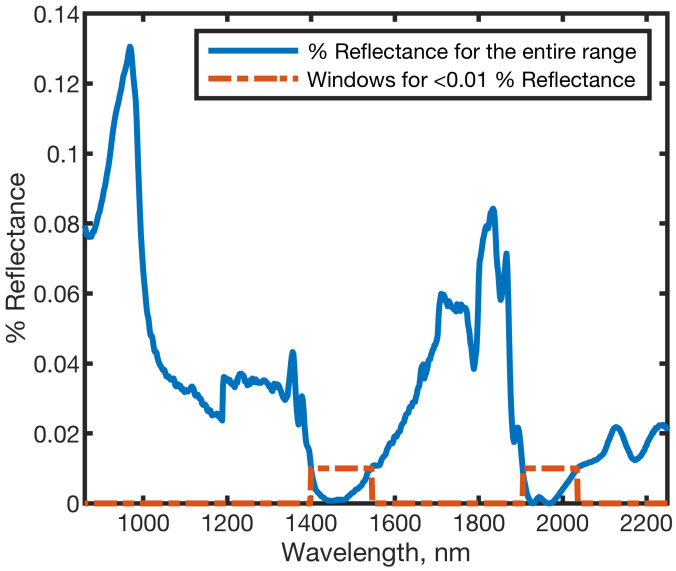


Fig. 6: Reflected power when light is entered from water to the *sciatic* nerve bundle. The dotted line indicates the wavelength ranges that offer the minimum (less than 0.01%) reflectance.

optical power lost in the medium due to the optical absorbance and a higher value of $k$ represents a higher absorbance. It is evident from fig. 5 (middle) that the *Sciatic* nerve sample has negligible $k$ for the wavelengths in the NIR region of spectrum up to $1380\ nm$, the value increases beyond that wavelength considerably. There are two distinct local maxima at $1480\ nm$ and $1980\ nm$ with the later corresponding to higher values for $k$. From a broader perspective, for $1400 - 1580\ nm$ and $1700 - 2050\ nm$ the nerve exhibits higher values of $k$, thereby making these two wavelength ranges the potentially preferred wavelengths for raising the nerve temperature by optical heating. It is therefore evident that wavelengths $> 1480$ are suitable for optical stimulation due to their suitability for effecting localised heating. Still, the choice of the operating wavelength also depends on other factors that will be discussed later in the section. Amongst the above mentioned two wavelength ranges, the second one has the potential to increase the local temperature at a higher pace while the first range can be useful if a more uniform heat distribution in the medium is required.

The $n$ and $k$ are two useful parameters of any medium for assessing optical wave propagation through it, theoretically or through simulations. The imaginary part of the refractive index ($k$), however, can be used to obtain the absorption coefficient ($\alpha$) of any medium, which is an even better indicator for optical absorption within the medium. The absorption coefficient $\alpha$ as given in equation (2), expressed in $cm^{-1}$, is related to the imaginary part of the refractive index ($k$). Figure 5 (bottom) shows the absorption coefficient ($\alpha$) calculated from $k$ using equation (2) over the $\lambda$ range. The graph is very similar to that of $k$, showing similar trends in characteristics over $\lambda$, with a slightly lower rate of increase with $\lambda$. For the range $\lambda < 1380\ nm$ the absorption coefficient, $\alpha \approx 10\ cm^{-1}$. There are two distinct peaks at $\lambda = 1380\ nm$ and $\lambda = 1980\ nm$ with $\alpha$ equals to $38\ cm^{-1}$ and $55\ cm^{-1}$ respectively. For the range $1480\ nm < \lambda < 1580\ nm$ and $1700\ nm < \lambda < 2050\ nm$ the overall $\alpha$ is significantly higher than the surroundings, making them potential candidates for optical nerve stimulator wavelengths. A higher $\alpha$ represents higher absorption in the medium and higher temperature rise in the medium. The second $\lambda$ range is more suitable for the case when a rapid temperature rise is desired. The trace of Fig. 5 (bottom) is redrawn in Fig. 7 with the windows around these ranges clearly identified using FWHM (Full Width at Half Maxima) around the peaks at $\lambda = 1380\ nm$ and $\lambda = 1980\ nm$. A higher value of $\alpha$ also reduces the penetration depth at which the optical power can be reached to affect the target nerve. Considering only the penetration depth the first range will allow the optical stimulus to reach deeper into the nerve bundle. If we aim to reach deeper into the medium, the $\alpha$ has to be minimized, however, if we wish to have a rapid temperature rise in the nerve tissue, the $\alpha$ has to be higher. Therefore, the choice of the wavelength is dependent on a number of factors i.e. how fast we wish to raise the temperature, how deep we wish to reach, how equalized we wish the temperature distribution within the nerve medium be. If the stimulation application calls for the targeting of a nerve fibre located near the surface of the nerve bundle and if a rapid rise in the local temperature is required, a wavelength in the range $1700\ nm < \lambda < 2050\ nm$ can be useful.

On the other hand, if it is desirable to elevate the overall temperature of a surface fibre without overheating at a very narrow localised tissue area, the range $1480\ nm < \lambda < 1580\ nm$ can be useful. By using any wavelength from that range it is also possible to reach deeper into the nerve bundle. An optical signal propagating through any lossy medium gets absorbed by the medium and as result its intensity reduces exponentially as described by equation (4). The rate of reduction in the intensity is higher in the case of a material with higher absorption coefficient ($\alpha$). A higher $\alpha$ in turn reduces the penetration depth ($\frac{1}{\alpha}$) into the material, defined as the depth at which the optical intensity reaches about 36% of its initial value.

To reach nerve fibres located deeper in the nerve bundle $\alpha$ has to be minimized. The solid trace in Figure 8 shows the calculated penetration depth ($\frac{1}{\alpha}$) resulting from the experimental data for the wavelengths $860 - 2250\ nm$ averaged over the *Sciatic* nerve samples used in this study.

There is one large maximum in the $\lambda$ range at $980\ nm$, where the optical power can reach at a depth of $2200\ \mu m$. However, considering the fact that most of the nerve bundles are $1000 - 2000\ \mu m$ in diameter, a penetration depth of $500 - 1000\ \mu m$ is sufficient to reach a fibre located at the centre of the nerve bundle. From fig. 8 it is clear that in the range $1700\ nm < \lambda < 2050\ nm$ the signals can reach a depth of $\approx 200 \mu m$ from the nerve surface and in $1480\ nm < \lambda < 1580\ nm$ a penetration depth of $300\ \mu m$ is possible. In the wavelengths of interest, the maximum depth where the optical signal can reach with sufficient intensity is about $300\ \mu m$. If it is required to reach beyond $300\ \mu m$, a mechanism has to be developed so that the localized intensity at the point of interest gets increased.

Myelin (in myelinated fibres) has been reported to contain

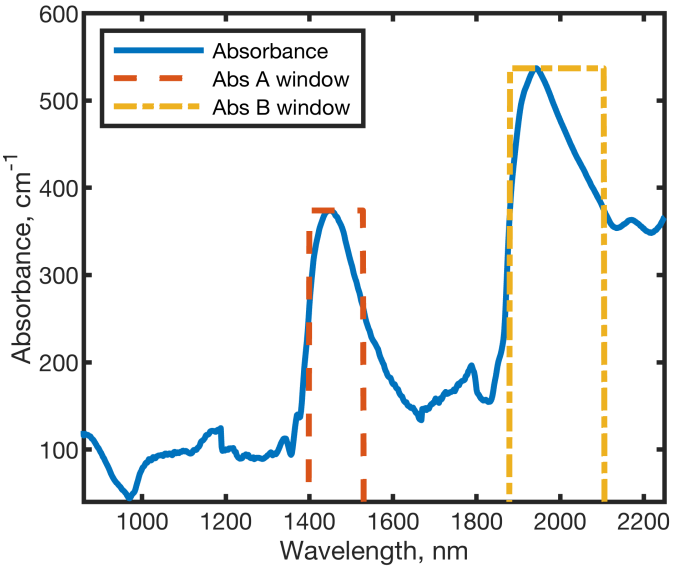


Fig. 7: Optimum wavelength ranges for maximising the absorption coefficient, $\alpha$. The curve is the same as the bottom trace of Fig. 5 with the widths of the windows A and B determined by the FWHM around the local maxima. These ranges are used in Fig. 10.

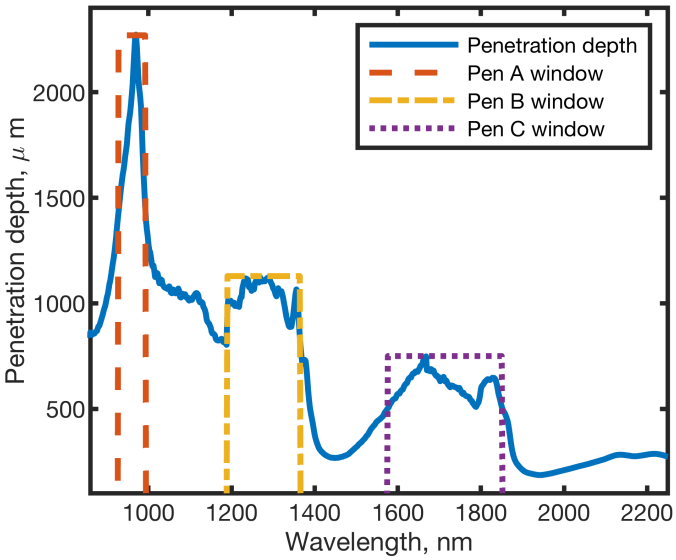


Fig. 8: Penetration depth for different wavelengths determined from spectroscopic measurements of the nerve. The windows A and B determined by the FWHM around the local maxima.

40% water and out of the remaining 60%, 80% is lipids and 20% is protein [35]. This makes the Water:Lipids:Protein ratio to be $40:48:12$. The previous studies only considered water absorption, hence, the total absorption should theoretically be 40% that of pure water absorption, considering the lipids and proteins are lossless. Our measurements on the total nerve tissue showed that the total absorption is more than 40% of the value corresponding to pure water. This result indicates that the lipids and proteins in the nerve are not completely lossless in optical frequencies, although they have lower absorption coefficients than the pure water. That means we need to launch more optical power from the laser so that the required power at the nerve membrane is reached for activation or blocking. There are challenges in obtaining the imaginary part of the refractive index experimentally, where the sample has finite thickness and scattering properties. Traditionally, the imaginary part of the refractive index can be obtained from the absorbance ($A$), which uses the Beer-Lambert law [26]. In this method, the Transmittance ($T$) is determined by using a spectrophotometer, and the absorbance can be determined by the following equation. The $k$ obtained by this method is labelled as $k_{BLT}$ in this paper.

$$k_{BLT} = -\frac{ln(T)\lambda}{4\pi} \tag{10}$$

As some light is reflected from the first interface of the sample, the $k$ value obtained in this way is not accurate. To eliminate the effects of reflection in calculating $k$, in [26], the authors used a modified equation for $A$, which is given in the following equation, and the $k$ thus obtained is labelled as $k_{BL}$.

$$k_{BL} = -\frac{ln(T+R)\lambda}{4\pi} \tag{11}$$

The method above eliminates the effect of the first reflection to some degree and produces a better estimation for $k$. A different approach was presented in [27], where the optical constants of silica glass were determined, taking the reflections from the interfaces into consideration. The calculated $k$ in that technique is labelled as $k_{calc}$.

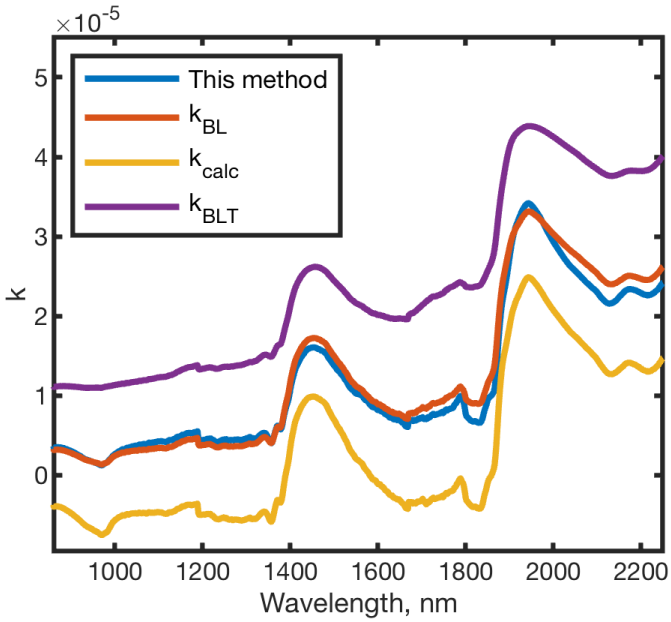


Fig. 9: Comparison of k calculated with different methods. $k_{BLT}$ ignores the reflection from the first interface and the nerve medium has infinite thickness. $k_{BL}$ considers the reflection from the first interface but ignores the finite thickness of the sample. $k_{calc}$ takes the finite thickness and the reflection into considerations. The method used in this article uses an iterative method to determine the value of $k$ for a given $T$, $R$ and user-defined error tolerance.

The method used here to estimate $k$ uses the fact that the incident light can have a reflection from the first interface of the sample and there can be multiple reflections within the sample before the light reaches the detector of the spectrophotometer. Figure 9 shows the obtained $k$ values for all the methods stated above over the entire wavelength range used in this study. It is evident from the result that $k_{BLT}$ gives a much higher estimate, $k_{calc}$ estimates a much lower value, however, $k_{BL}$ and our method give similar estimations. As our method considers the reflections, the finite thickness of the sample and uses a iterative method to converge toward a value, which is the theoretical value for a given $R$ and $T$,the method used in this study is expected to produce more accurate values.

### A. *Choice of wavelengths for different stimulation types*

As mentioned earlier, an Optical Nerve stimulation system is expected to be able to apply the appropriate stimulus to either activate, inhibit or block neural activity. Moreover, fascicle (i.e. spatial) selectivity is often desirable to allow either of these types of stimuli to be applied to a neuron that is located at a specific depth inside a nerve bundle. These types of neurostimulation selectivity are related to three main optical parameters that can be derived from the work presented in this paper: reflection, absorbance and penetration depth. Still, it is evident from the first section of this paper that the choice of wavelengths in the literature has not previously taken these parameters into consideration, but has rather been mostly based on available optical sources designed for other applications.

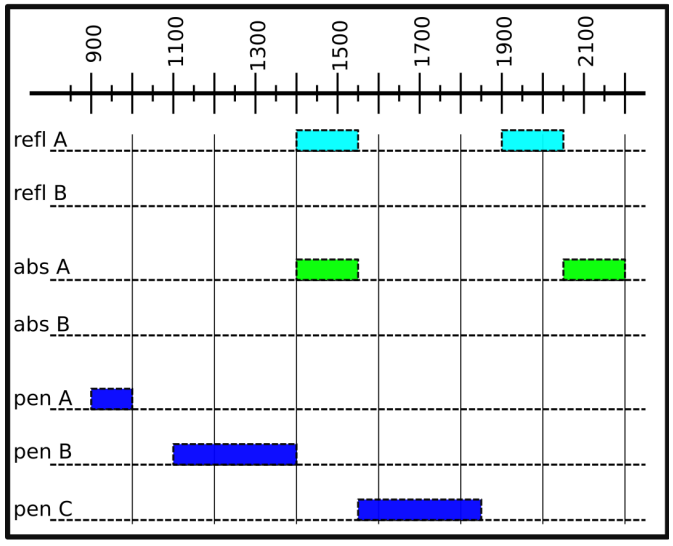


Fig. 10: Wavelengths that can be potentially used for optical neurostimulation offering either minimum reflected power (denoted "refl"), maximum absorbance (abs) or different penetration depths (decreasing from pen A to pen C).

The appropriate wavelengths that can be chosen for specifying the appropriate type of optical neurostimulation to be used according to the desirable outcome are summarised in Fig. 10. It indicates the desirable wavelength ranges for each of the neural tissue parameters including Reflection from the nerve bundle boundary (denoted "refl" - ranges indicated in Fig. 6); Absorbance within the nerve bundle ("abs" from Fig. 7); and Penetration depths of the optical signal inside the nerve bundle ("pen" from Fig. 8).

From the perspective of minimising losses, two wavelength ranges were identified (refl-A and B) where the reflection is minimal ($< 0.01\%$) allowing most of the incident power to enter the nerve. In terms of the stimulation outcome, blocking neural activity can be best achieved through the gradual rise and prolonged retention of a specific temperature level, while for nerve activation a rapid and brief increase in localised temperature is required. For either of these applications two wavelength ranges are identified in fig. 10 for maximizing absorbance, abs-A and B respectively, each potentially allowing for different rates of change of temperature. The use of wavelengths at the area of abs-A (around $1490$ nm), where the absorption peak is smaller than that of abs-B, will allow the temperature distribution within the nerve to increase more gradually, allowing the targeted tissue more time to dissipate the heat through diffusion and convection. At the region of abs-B (around $1980$ nm), where the absorption coefficient is the highest in the wavelength range of this study, a short duration, and high-intensity optical pulse would create a high-temperature gradient. Thus this paper suggests the $1490$ nm wavelength as the optimum choice for blocking or inhibition, and a short and high amplitude pulse at $1980$ nm as optimum for neural activation. Finally, three regions of wavelengths (pen-A, B and C) are indicated in fig. 10 as suitable for allowing the optical power to reach specific depths (around 2mm, 1mm and 0.5mm respectively) inside the nerve bundle. The appropriate selection could facilitate fascicle selectivity, i.e. the distinct stimulation of deep fibres and superficial fibres separately.

## IV. Conclusions

Given an increasing interest in optical nerve stimulation, the previously unmet need to determine how optical parameters affect neural tissue was addressed experimentally and through simulations in this paper. Studies in the field have been using a range of wavelengths to demonstrate peripheral nerve stimulation using light, with these wavelengths being selected empirically or with a certain degree of ambiguity. Here, the complex refractive index of the sciatic nerve of *Xenopus laevis* was determined for the first time and optimum wavelengths are proposed for optimising the potential therapeutic effects of infrared nerve stimulation. The scope of this paper was to determine the optical properties of the Xenopus laevis sciatic nerve, as it is the most common neural tissue used in peripheral neurostimulation ex-vivo experiments. The authors' intention was not to create an all encompassing reference. As such additional nerve diameters, tissue inhomogeneity effects or tissue samples from other species, although useful, were outside the aim of this work.

After acquiring spectrophotometric data from an ex-vivo nerve sample, a method other than the Beer-Lambert law was used to calculate the optical constants (real and imaginary parts of the refractive index). Our method takes the reflections

from outside and within the sample into account and the finite thickness of the sample is also taken into consideration. A Newton's iterative method is used to calculate the optical constants for the Reflectance ($R$) and Transmittance ($T$) from the spectrophotometer thus improving the accuracy of the result.

Using the optical constants, the reflected power from the nerve interface is calculated and the optimum wavelength range where the reflected power is minimised was identified. Similarly, the absorbance characteristics of neural tissue were determined and the optimum wavelength where the optical absorption is maximised was identified. Finally, the penetration depth of optical stimuli was determined for the entire wavelength range considered and several suitable localised ranges were identified, that would be beneficial for optical stimulation of deep fibres.

Thus, the optimum wavelengths that can be used for optical stimulation of peripheral nerves either for nerve activation, for inhibition or for blocking were identified.

## ACKNOWLEDGMENT

The authors would like to thank *EPSRC* (Grant ref.: EP/N008499/1) for supporting the work and Prof. Ronald Douglas, City, University of London, for the invaluable support and advice.

## REFERENCES

[1] E. J. Bradbury, L. D. Moon, R. J. Popat, V. R. King, G. S. Bennett, P. N. Patel, J. W. Fawcett, and S. B. McMahon, "Chondroitinase abc promotes functional recovery after spinal cord injury," *Nature*, vol. 416, no. 6881, p. 636, 2002.

[2] F. Fregni, P. S. Boggio, M. C. Lima, M. J. Ferreira, T. Wagner, S. P. Rigonatti, A. W. Castro, D. R. Souza, M. Riberto, S. D. Freedman, *et al.*, "A sham-controlled, phase ii trial of transcranial direct current stimulation for the treatment of central pain in traumatic spinal cord injury," *Pain*, vol. 122, no. 1-2, pp. 197–209, 2006.

[3] N. Hoshimiya, A. Naito, M. Yajima, and Y. Handa, "A multichannel fes system for the restoration of motor functions in high spinal cord injury patients: a respiration-controlled system for multijoint upper extremity," *IEEE Trans. Biomed. Eng.*, vol. 36, no. 7, pp. 754–760, 1989.

[4] H. H. Müller, S. Moeller, C. Lücke, A. P. Lam, N. Braun, and A. Philipsen, "Vagus nerve stimulation (vns) and other augmentation strategies for therapy-resistant depression (trd): Review of the evidence and clinical advice for use," *Front. neurosci.*, vol. 12, p. 239, 2018.

[5] D. R. Merrill, M. Bikson, and J. G. Jefferys, "Electrical stimulation of excitable tissue: design of efficacious and safe protocols," *Journal of neuroscience methods*, vol. 141, no. 2, pp. 171–198, 2005.

[6] C. Tai, W. C. De Groat, and J. R. Roppolo, "Simulation analysis of conduction block in unmyelinated axons induced by high-frequency biphasic electrical currents," *IEEE Trans. Biomed. Eng.*, vol. 52, no. 7, pp. 1323–1332, 2005.

[7] A. Guilvard, A. Eftekhar, S. Luan, C. Toumazou, and T. G. Constandinou, "A fully-programmable neural interface for multi-polar, multi-channel stimulation strategies," in *IEEE ISCAS, 2012*, pp. 2235–2238, IEEE, 2012.

[8] J. H. Kim, J. B. Davidson, O. Röhrle, T. K. Soboleva, and A. J. Pullan, "Anatomically based lower limb nerve model for electrical stimulation," *Biomedical engineering online*, vol. 6, no. 1, p. 48, 2007.

[9] G. Loeb and R. Peck, "Cuff electrodes for chronic stimulation and recording of peripheral nerve activity," *Journal of neuroscience methods*, vol. 64, no. 1, pp. 95–103, 1996.

[10] F. Wu, E. Stark, M. Im, I.-J. Cho, L. Tien, F. Chen, E.-S. Yoon, G. Buzsaki, D. Kaplan, J. Berke, *et al.*, "Implantable neural probes for chronic electrical recording and optical stimulation," in *Electron Devices Meeting (IEDM), 2013 IEEE International*, pp. 8–6, IEEE, 2013.

[11] I. F. Triantis, A. Demosthenous, and N. Donaldson, "On cuff imbalance and tripolar eng amplifier configurations," *Biomedical Engineering, IEEE Transactions on*, vol. 52, no. 2, pp. 314–320, 2005.

[12] D. Tepper, "Transcutaneous supraorbital neurostimulation (tsns)," *Headache: The Journal of Head and Face Pain*, vol. 54, no. 8, pp. 1415–1416, 2014.

[13] H.-M. Lee, K. Y. Kwon, W. Li, and M. Ghovanloo, "A power-efficient switched-capacitor stimulating system for electrical/optical deep brain stimulation," *IEEE J. Solid-State C.*, vol. 50, no. 1, pp. 360–374, 2015.

[14] Y. Kobayashi, K. Oshima, and I. Tasaki, "Analysis of afferent and efferent systems in the muscle nerve of the toad and cat," *The Journal of physiology*, vol. 117, no. 2, p. 152, 1952.

[15] C. A. Miller, P. J. Abbas, C. J. Brown, *et al.*, "An improved method of reducing stimulus artifact in the electrically evoked whole-nerve potential," *Ear and hearing*, vol. 21, no. 4, pp. 280–290, 2000.

[16] O. Yizhar, L. E. Fenno, T. J. Davidson, M. Mogri, and K. Deisseroth, "Optogenetics in neural systems," *Neuron*, vol. 71, no. 1, pp. 9–34, 2011.

[17] A. R. Duke, J. M. Cayce, J. D. Malphrus, P. Konrad, A. Mahadevan-Jansen, and E. D. Jansen, "Combining electrical and optical techniques to develop a novel modality for neural activation," in *Biomed. Sci. Eng. Conf. (BSEC), 2010*, pp. 1–4, IEEE, 2010.

[18] A. R. Duke, E. Peterson, M. A. Mackanos, J. Atkinson, D. Tyler, and E. D. Jansen, "Hybrid electro-optical stimulation of the rat sciatic nerve induces force generation in the plantarflexor muscles," *Journal of neural engineering*, vol. 9, no. 6, p. 066006, 2012.

[19] A. R. Duke, M. W. Jenkins, H. Lu, J. M. McManus, H. J. Chiel, and E. D. Jansen, "Transient and selective suppression of neural activity with infrared light," *Scientific reports*, vol. 3, 2013.

[20] J. Zhang, F. Laiwalla, J. A. Kim, H. Urabe, R. Van Wagenen, Y.-K. Song, B. W. Connors, and A. V. Nurmikko, "A microelectrode array incorporating an optical waveguide device for stimulation and spatiotemporal electrical recording of neural activity," in *Engineering in Medicine and Biology Society, 2009. EMBC 2009. Annual International Conference of the IEEE*, pp. 2046–2049, IEEE, 2009.

[21] J. Wells, C. Kao, P. Konrad, T. Milner, J. Kim, A. Mahadevan-Jansen, and E. D. Jansen, "Biophysical mechanisms of transient optical stimulation of peripheral nerve," *Biophysical journal*, vol. 93, no. 7, pp. 2567–2580, 2007.

[22] Z. Mou, I. F. Triantis, V. M. Woods, C. Toumazou, and K. Nikolic, "A simulation study of the combined thermoelectric extracellular stimulation of the sciatic nerve of the xenopus laevis: the localized transient heat block," *Biomedical Engineering, IEEE Transactions on*, vol. 59, no. 6, pp. 1758–1769, 2012.

[23] M. G. Shapiro, K. Homma, S. Villarreal, C.-P. Richter, and F. Bezanilla, "Infrared light excites cells by changing their electrical capacitance," *Nature communications*, vol. 3, p. 736, 2012.

[24] S. Luan, I. Williams, K. Nikolic, and T. G. Constandinou, "Neuromodulation: present and emerging methods," *Frontiers in neuroengineering*, vol. 7, p. 27, 2014.

[25] A. J. Saubermann and V. L. Scheid, "Elemental composition and water content of neuron and glial cells in the central nervous system of the north american medicinal leech (macrobdella decora)," *Journal of Neurochemistry*, vol. 44, no. 3, pp. 825–834, 1985.

[26] T. G. Mayerhöfer, H. Mutschke, and J. Popp, "Employing theories far beyond their limits—the case of the (boguer-) beer–lambert law," *ChemPhysChem*, vol. 17, no. 13, pp. 1948–1955, 2016.

[27] R. Kitamura, L. Pilon, and M. Jonasz, "Optical constants of silica glass from extreme ultraviolet to far infrared at near room temperature," *Applied optics*, vol. 46, no. 33, pp. 8118–8133, 2007.

[28] S. Ringer, "Regarding the action of hydrate of soda, hydrate of ammonia, and hydrate of potash on the ventricle of the frog's heart," *The Journal of physiology*, vol. 3, no. 3-4, pp. 195–202, 1882.

[29] R. Phillips, "A numerical method for determining the complex refractive index from reflectance and transmittance of supported thin films," *Journal of Physics D: Applied Physics*, vol. 16, no. 4, p. 489, 1983.

[30] M.-H. Chiu, J.-Y. Lee, and D.-C. Su, "Complex refractive-index measurement based on fresnel's equations and the uses of heterodyne interferometry," *Applied optics*, vol. 38, no. 19, pp. 4047–4052, 1999.

[31] F. Padera, "Measuring absorptance (k) and refractive index (n) of thin films with the perkinelmer lambda 950/1050 high performance uv-vis/nir spectrometers," *PerkinElmer Inc.: App. note: UV/Vis Spectroscopy*, 2013.

[32] M. A. Almadi, "Optical properties measurements of rat muscle and myocardium at 980 and 1860 nm using single integrating sphere technique," 2014.

[33] W. Jiang, M. Almadi, N. Salas, and S. Rajguru, "Optical properties of biological tissues measured at infrared wavelengths," in *Biomedical Optics*, pp. BT3A–42, Optical Society of America, 2014.

[34] J. Nocedal and S. J. Wright, *Nonlinear Equations*. Springer, 2006.

[35] S. L. Jacques, "Optical properties of biological tissues: a review," *Physics in medicine and biology*, vol. 58, no. 11, p. R37, 2013.